




## Article

# Mechanical Properties and Microstructural Behavior of Uniaxial Tensile-Loaded Anisotropic Magnetorheological Elastomer

Siti Fatimah Mohd Shahar <sup>1</sup>, Saiful Amri Mazlan <sup>1,\*</sup> , Norhasnidawani Johari <sup>1</sup>, Mohd Aidy Faizal Johari <sup>1</sup> , Siti Aishah Abdul Aziz <sup>2</sup> , Muntaz Hana Ahmad Khairi <sup>1</sup>, Nur Azmah Nordin <sup>1</sup> and Norhiwani Mohd Hapipi <sup>3</sup>

<sup>1</sup> Engineering Materials & Structures (eMast) ikohza, Malaysia-Japan International Institute of Technology (MJIT), Universiti Teknologi Malaysia, Kuala Lumpur 54100, Malaysia

<sup>2</sup> Faculty of Applied Sciences, Universiti Teknologi MARA (UiTM) Cawangan Pahang, Bandar Tun Abdul Razak Jengka 26400, Malaysia

<sup>3</sup> Physics Department, Center for Foundation Studies in Science, Universiti Malaya, Kuala Lumpur 50603, Malaysia

\* Correspondence: amri.kl@utm.my

**Abstract:** Magnetorheological elastomers (MREs) are well-known for their ability to self-adjust their mechanical properties in response to magnetic field influence. This ability, however, diminishes under high-strain conditions, a phenomenon known as the stress-softening effect. Similar phenomena have been observed in other filled elastomers; hence, the current study demonstrates the role of fillers in reducing the effect and thus maintaining performance. Anisotropic, silicone-based MREs with various carbonyl iron particle (CIP) concentrations were prepared and subjected to uniaxial tensile load to evaluate high-strain conditions with and without magnetic influence. The current study demonstrated that non-linear stress–strain behavior was observed in all types of samples, which supported the experimental findings. CIP concentration has a significant impact on the stress–strain behavior of MREs, with about 350% increased elastic modulus with increasing CIP content. Microstructural observations using field emission scanning electron microscopy (FESEM) yielded novel micro-mechanisms of the high-strain failure process of MREs. The magnetic force applied during tension loading was important in the behavior and characteristics of the MRE failure mechanism, and the discovery of microcracks and microplasticity, which was never reported in the MRE quasi-static tensile, received special attention in this study. The relationships between these microstructural phenomena, magnetic influence, and MRE mechanical properties were defined and discussed thoroughly. Overall, the process of microcracks and microplasticity in the MRE under tensile mode was primarily formed in the matrix, and the formation varies with CIP concentrations.

**Keywords:** anisotropic; magnetorheological elastomers; microcracks; microplasticity; morphology; Mullins effect; tension



**Citation:** Mohd Shahar, S.F.; Mazlan, S.A.; Johari, N.; Johari, M.A.F.; Abdul Aziz, S.A.; Ahmad Khairi, M.H.; Nordin, N.A.; Mohd Hapipi, N. Mechanical Properties and Microstructural Behavior of Uniaxial Tensile-Loaded Anisotropic Magnetorheological Elastomer. *Actuators* **2022**, *11*, 306. <https://doi.org/10.3390/act11110306>

Academic Editor: Ramin Sedaghati

Received: 10 September 2022

Accepted: 25 October 2022

Published: 26 October 2022

**Publisher's Note:** MDPI stays neutral with regard to jurisdictional claims in published maps and institutional affiliations.



**Copyright:** © 2022 by the authors. Licensee MDPI, Basel, Switzerland. This article is an open access article distributed under the terms and conditions of the Creative Commons Attribution (CC BY) license (<https://creativecommons.org/licenses/by/4.0/>).

## 1. Introduction

The magnetorheological elastomers (MREs) are gaining popularity due to their fascinating ability to change mechanical properties continuously, rapidly, and even reversibly in the presence of external magnetic stimuli [1–10]. This unique property has piqued the interest of researchers because it is useful for many advanced technologies, and it has allowed them to be classified as ‘smart materials’. Before selecting a material for an engineering product or application, it is necessary to understand the mechanical properties of the material to determine its range of usefulness and predict its service life. Furthermore, any potential damages can be predicted and controlled for future use. Several studies on a variety of working modes, such as tension mode [11–15], compression mode [16,17], and shear mode [18–21], have been conducted for obtaining the mechanical properties of MREs. The properties, particularly the stress–strain relationship of the applied magnetic field, have been evaluated in a linear viscoelastic (LVE) region, with only minor strain applied

throughout the test. Essentially, by applying the maximum loading to the MREs during the test, the study could be expanded to a broader region of the respective strain.

An actuator is a device that causes something to move or operate. The movement can be linear or rotary. In terms of movement pattern, this current study contributes to a better understanding of the materials' responses to linear movement. Because the materials (MREs) used in this study have the potential to be used in actuators, the characteristic toward linear movement can be related to the phenomena observed in the investigation. The central concept of actuator design is how input energy can be converted into physical or mechanical energy capable of moving something. Electric motors, hydraulic motors, and pneumatic control valves are popular examples of input energy available today. The challenges of designing actuators become even more critical as the size is reduced, resulting in a demand for miniaturized soft actuators that respond to various stimuli and exhibit deformations. Along with the exciting advances in artificial intelligence technology, actuators should be made of smart materials that can fulfill the demand of stimulation. Again, relevant to this study, MREs are one of the best examples that can be applied as magnetic responsive actuators. Furthermore, magnetic actuators have been reported [22] to have been used successfully in the development of various crawling devices, swimmers, and micropumps.

Several studies [2,12,13] found that MREs exhibited a slight weakening in mechanical performance at maximum strain, known as the stress-softening effect, and this phenomenon was rarely reported and discussed, highlighting the need for further research. This stress-softening effect is highly sensitive to all filled-rubber materials. The first discovery was made by Mullins who discovered that stretching vulcanized rubber containing fillers significantly altered the properties of the rubber due to the breakdown of both agglomerates and chains of the filler particles, as well as the adsorption of the filler particles on the rubber. Later, Diani et al. [23] provided a comprehensive review of Mullins' works. The study concluded that this phenomenon occurred most frequently during the first deformation of the rubber and was associated with residual strain, and theories, such as bond rupture, molecule slipping, filler cluster rupture, and chain disentanglement, were developed to explain the effect. However, there is no data on the extensive relationship between the phenomena at high-strain performance and the microstructure behavior of MREs in tension mode in the literature.

A thorough investigation of the microstructure behavior of MRE materials is required to comprehend how specific phenomena affect the properties of MREs and influence the microstructure behavior as occurred in other composite materials [24–28]. The majority of MRE microstructure studies focused on pre-structural [29,30] particle arrangements in the matrix [31,32] and small-strain deformation [5,33,34]. Johari et al. [35] revealed the development of permanent microplasticity in MRE samples subjected to small-shear deformation, which reduced the MRE's ability to store energy. Again, the extent to which stress and strain influence MRE microstructure during large strain is unknown. In fact, the morphological aspects of MREs subjected to tensile mode were never discussed. Forensic investigation of the failure mechanism on tensile-loaded surfaces is critical and will undoubtedly contribute to the current literature. Microstructural observations using advanced microscopy instruments reveal novel micro-mechanisms of the MREs undergoing uniaxial tensioning, and this mechanism will be more distinctive as the MREs are responsive to magnetic stimulation during the test, which plays an important role in the behavior and characteristics of the MRE failure mechanism.

To fill a gap in the literature, this study investigates the softening effect and its relationship to microscopic evidence of anisotropic, silicone-based MREs by varying magnetic particle volume concentrations. The stress–strain behavior of the MREs was examined in both the absence and presence of a magnetic field. The influence of particle concentration and magnetic influence on the mechanical properties and microstructural phenomena of the failed silicone-based MREs under uniaxial tensile-loading conditions is discussed in

detail in this study. The failure mechanism was then proposed to explain the phenomenon and its relationship to microscopic behavior.

## 2. Materials and Methods

### 2.1. Sample Preparation

The matrix was the two-component RTV silicone rubber NS625A supplied by Nippon Steel Co., Tokyo, Japan, and the ferromagnetic filler used in this study was carbonyl iron particles (CIPs), OM grade having an average particle size of 3–6  $\mu\text{m}$  provided by BASF, Ludwigshafen, Germany. The curing agent, NS625B, obtained from Nippon Steel Co., Japan was used as a crosslinking agent. Three types of samples were fabricated, namely pure silicone rubber (SR), MREs with 10 vol.% CIPs (10MREs), and MREs with 20 vol.% CIPs (20MREs). The pure SR was made by adding 2% curing agent to an SR solution and constantly mixing it. Meanwhile, for the MRE samples, the different volume concentrations of CIPs, 10 and 20 vol.%, were mixed thoroughly with the SR base using a mechanical stirrer with a speed of 200 rpm for 20 min at room temperature to ensure uniform distribution. Then, a curing agent was added and mixed into the homogenous mixture around 0.04% to 0.10% to allow the paste-like mixture to solidify and create cross-linking. Furthermore, the cross-linking process between the curing agent and the silicone rubber solution followed the established manufacturer's standard procedure and guidelines. Then, the sample was then poured into a closed, customized cylindrical steel mold with a diameter size of 50 mm with 1 mm thickness. To prepare anisotropic MRE samples, the mold was placed in the center of a solenoid coil that generated a 300 mT magnetic field for 30 min to allow particles to align with the flux direction before being left without magnetic stimulation for two hours to cure. Figure 1 depicts the illustration of the curing process. The beam-like anisotropic MRE sample with 35 mm length and 2 mm width then was cut from the MRE disc sheet using a sharp blade for uniaxial tension analysis (dimension as per ISO-37, type 4).

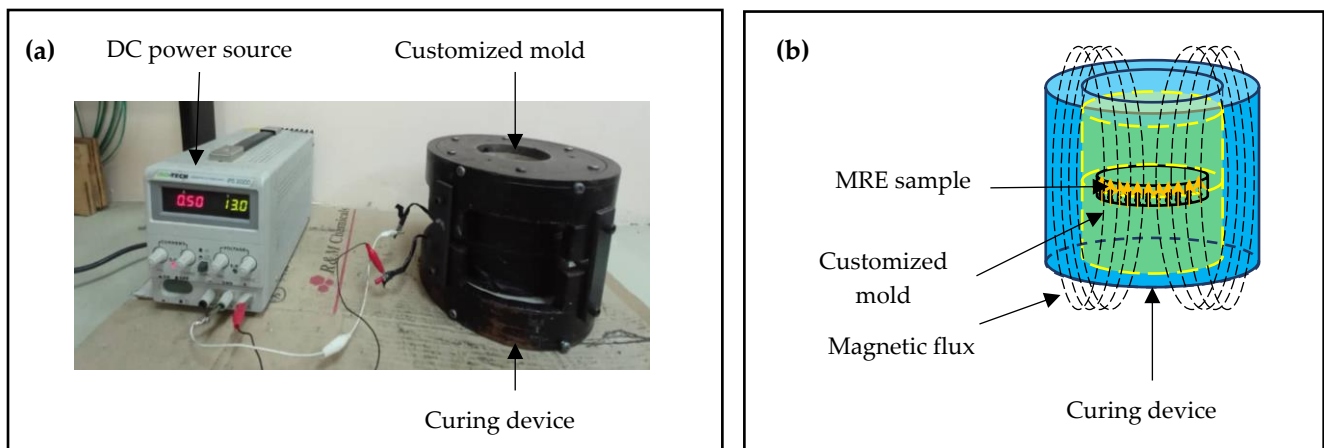


**Figure 1.** Optical images of anisotropic silicone-based MRE curing process: (a) real magnetic setup and (b) illustration of the magnetic flux inside the curing device.

### 2.2. Testing Method—Uniaxial Tension Testing

The quasi-static uniaxial tensile test was performed on a Universal Testing Machine (Shimadzu AGX-S, Kyoto, Japan) to analyze the large-strain behavior of anisotropic MREs during the absence (off state) and presence (on state) of the magnetic field. The beam-like shaped MRE sample was positioned parallel to the tensile load equipped with a load cell, as shown in Figure 2. During the on-state testing, a 0.2 T permanent magnet (Neodymium N52) supplied by One Magnet Electronic (M) Sdn. Bhd. was placed on both sides of the MRE samples, parallel with the alignment of the CIPs inside the sample. The reading taken by the Tesla meter indicated that the magnetic field in the testing area (gauge length) was 50 mT. This alignment was chosen to investigate the impact of the CIP alignment

on the MRE tensile strength. When the MRE sample is subjected to tensile force in the vertical direction, an equal and opposite force acts on the fixed end supplied by the CIP arrangement and magnetic field which resists the tensile loading, increasing the modulus.

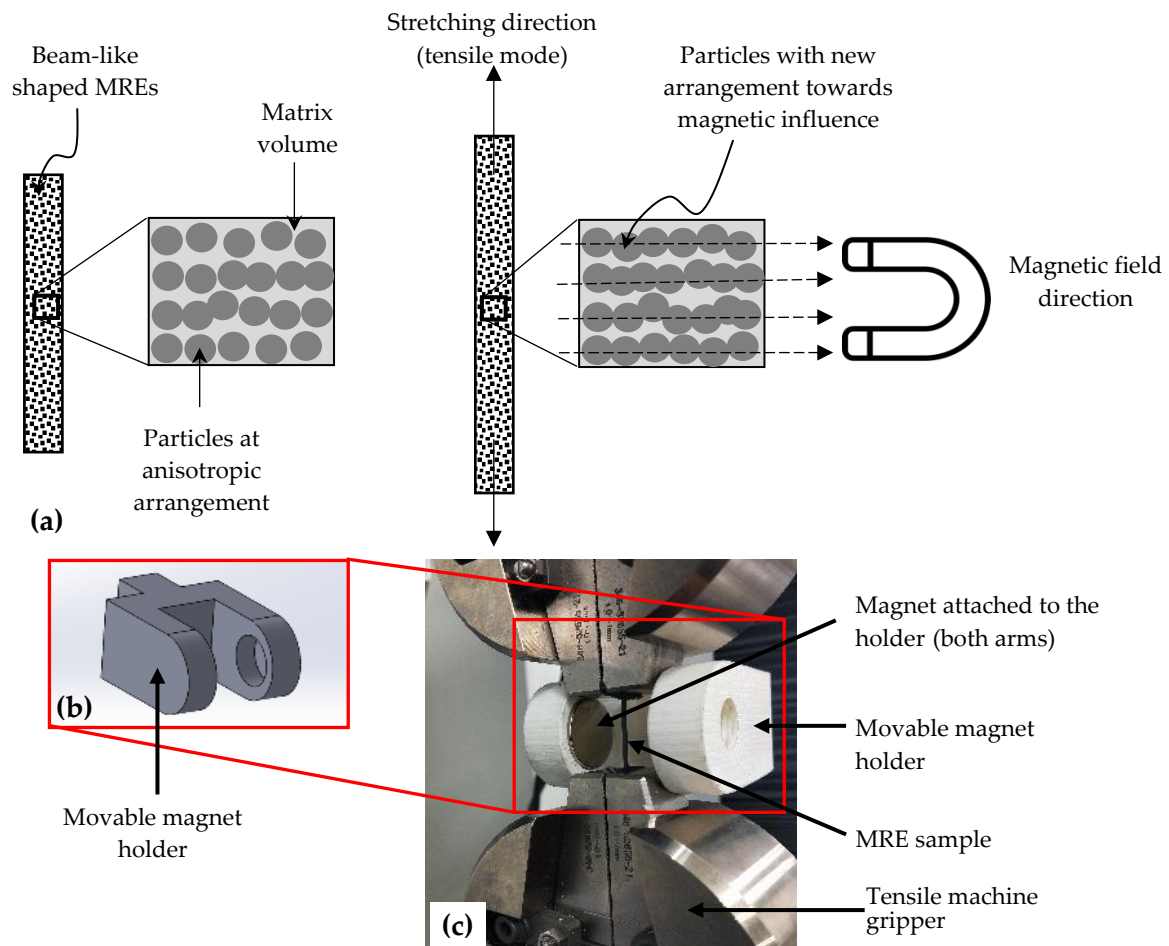


**Figure 2.** The test setup for quasi-static uniaxial tensile test is depicted: (a) schematic diagram explaining the direction of stretching (tension mode), CIP arrangement, and magnetic field; (b) movable magnet holder; (c) the magnetic setup with permanent magnet at 30 mm inter-magnet distance that produces 50 mT magnetic field.

A maximum length of the sample, 25 mm, with a gauge length of 10 mm was prepared for the testing. A movable magnet holder made from non-magnetic material, namely polylactic acid (PLA), was fabricated by using 3D printing, which was used to hold the magnet with an inter-magnet distance of 30 mm during the experimental procedure. Meanwhile, the magnet holder was used to ensure the amount of the induced magnetic field remained consistent throughout the experiment. The tensile machine gripper's upper parts were attached to the movable magnet holder. When the samples elongate, the magnet holder moves with them to keep the magnet position in the center of the gauge length area. The MRE samples were tested for uniaxial tension using an ASTM D412 procedure at a speed of 50 mm/min for both off- and on-state conditions at room temperature until the sample broke.

### 2.3. Morphology Analysis

Samples before and after the tensile test were cut into 1 mm × 10 mm straps with a sharp blade set at right angles near the fractured gauge length. The cut region was chosen with the understanding that any tensile deformation would have a greater effect on the sample's gauge length. MRE samples were collected for both before and after the tension

tests to compare microstructure characteristics and failure analysis. FESEM, JSM 7800F Prime model JOEL, Japan, was used to examine the cross-section of MRE samples. Before the evaluation, the samples were sputtered with gold in a vacuum chamber to improve the quality of the resulting images.

### 3. Results

#### 3.1. CIP Concentrations and Magnetic Field Influence

The stiffness and stress increases caused by the different CIP concentrations and alignment as well as the magnetic field inducement were investigated. Figure 3 depicts the stress–strain curves of pure SR and all MRE samples tested under tension mode at the off- and on-state conditions.

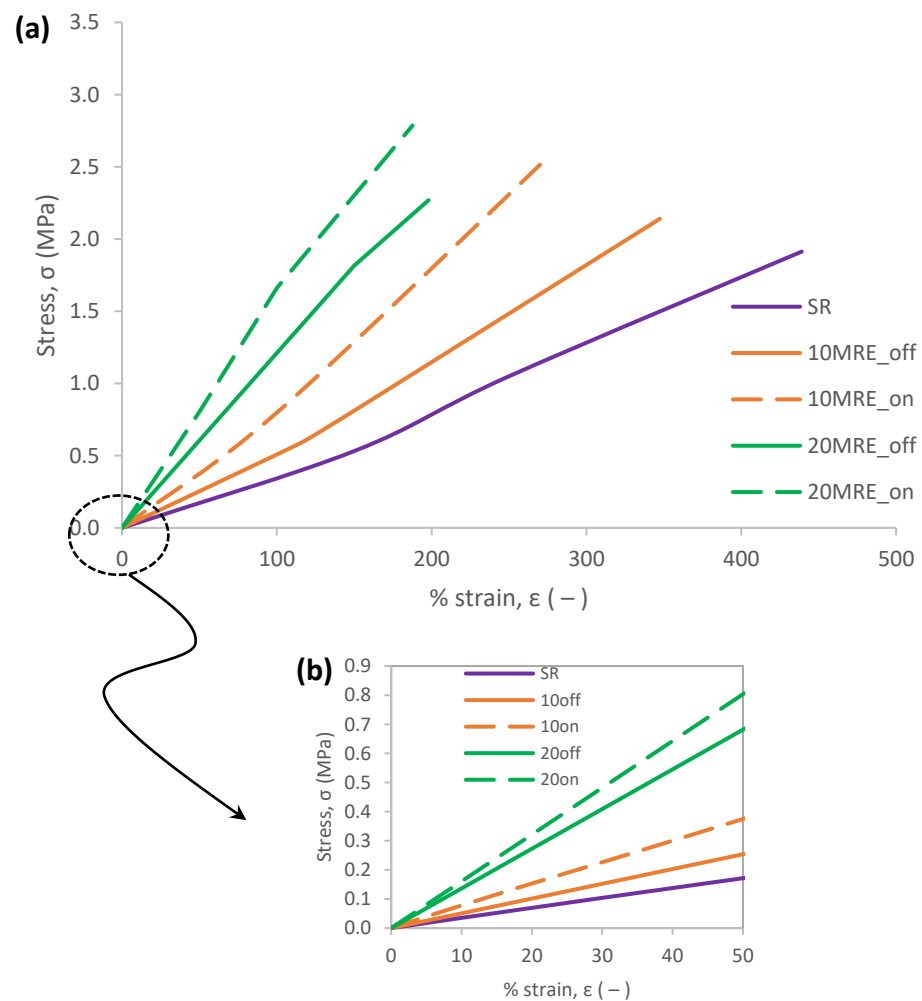


**Figure 3.** (a) Total strain and (b) magnification at 50% strain on stress–strain results of a quasi-static uniaxial tensile test of pure SR, MREs at 10 vol.%, CIPs and MREs at 20 vol.%, and CIPs with and without magnetic fields.

Non-linear stress–strain behavior was observed in all types of samples, correlating with previous reports [2,11,13]. At the first stage of the tensile test, all samples exhibited elastic behavior with a linear inclination pattern. Above 100% strain, all samples had non-uniform patterns of a linearity curve shape, with SR and 10MREs showing increasing slope and 20MREs showing decreasing slope. This is because 20MREs contain more particles. As a result, it carried more particles–particles and particles–matrix bonds (secondary interactions) than matrix–matrix bonds (primary interaction). This secondary interaction is weaker than the primary interaction, resulting in a shorter molecular chain. Consequently,

when the strain reached 100% for 20MRE, most of the shorter molecular chain was broken, leaving only the longer molecular chain. The small amount of the longer molecular chain will accommodate with less stress distributed along the chain. Surprisingly, the trend was consistent with CIP concentrations, as increasing the concentration increases sample stiffness, as evidenced by the gradient of the slope of the curve. It, however, reduced the tensile stress at break and as a result, the MRE sample's strength at failure. The trend held under both off- and on-state conditions.

Tension at magnetic inducement revealed that the tensile stress of MRE samples increased as the strain increased. The slope of the graphs indicated that the samples have higher stiffness when tested without magnetic field inducement. Because higher volume concentrations of CIPs result in higher stiffness and stresses where CIP concentration has a greater influence on this phenomenon. This result suggested that higher magnetic particle concentrations in MREs caused increases in Young's modulus. The difference between before and after the magnetic inducement was greater in the 10 vol.% MRE samples, which might be due to the strength of the magnetic field used.

Although the curves showed the same pattern of development, the stress–strain of MREs with 10 vol.% CIPs exhibited significant change in stress and strain during the off- and on-state conditions. This finding implied that applying 50 mT to the MREs during the tensile test has a significant impact on its behavior as it stiffens. On the other hand, the slope of the curve for MREs with 20 vol.% CIPs decreases with large deformation. This is due to the viscoelastic behavior of MRE material. As a result, there are certain changes in deformation when reaching large deformation. This is a common phenomenon for viscoelastic material with higher CIPs. However, the reduction of the slope is still substantially much higher than MREs with 10 vol.% CIPs and pure silicone rubber. Furthermore, the evaluation of the stiffness was evaluated at 100% strain (Refer to Figure 3b).

The stress–strain curves revealed that when the strain was small, the sample's tensile stress increased slowly with the strain (Figure 3b). The tensile stress of the MRE sample, on the other hand, increased exponentially as the strain increased. The stress output of the sample after adding the magnetic field was greater than the MRE sample before adding the magnetic field under the same strain. Furthermore, the modulus increased with CIP concentrations (Figure 4).

The particle magnetization was caused by the external magnetic field and the greater magnetization was caused by the higher concentration, indicating that the MRE internal force was more than just the restoring force of the rubber matrix. Nonetheless, the magnetic force between particles stimulated by an external magnetic field was directly proportional to the CIP concentrations, implying that the MRE sample has a definite magnetostrictive effect [36]. As a result, the external magnetic field and CIP concentrations can have significant impacts on mechanical properties.

### 3.2. Morphological Analysis

Figure 5 depicts the surface morphologies of anisotropic silicone-based MRE samples. The anisotropic MRE sample with 20 vol.% CIPs was found to have particle alignment, as shown in Figure 5a. The yellow arrow indicates the alignment direction in relation to the magnetic flux pattern used during the curing process. At low vol.% CIPs, however, the chain-like alignment was barely discernible. Because of the low concentration of CIPs, the interaction and attraction between the CIPs were slightly weaker (Figure 5b) in comparison to the higher CIP concentrations. In addition, MRE sample alignment at 10 vol.% could be noticeable for CIPs with smaller diameters. At 20 vol.% CIPs, however, the chain-like alignment was visible, and more protruded CIPs were seen distributed throughout the sample. As a result, at higher CIP concentrations, MRE samples have better particle–particle interactions, which were responsible for the formation of chain-like structures during the curing process.

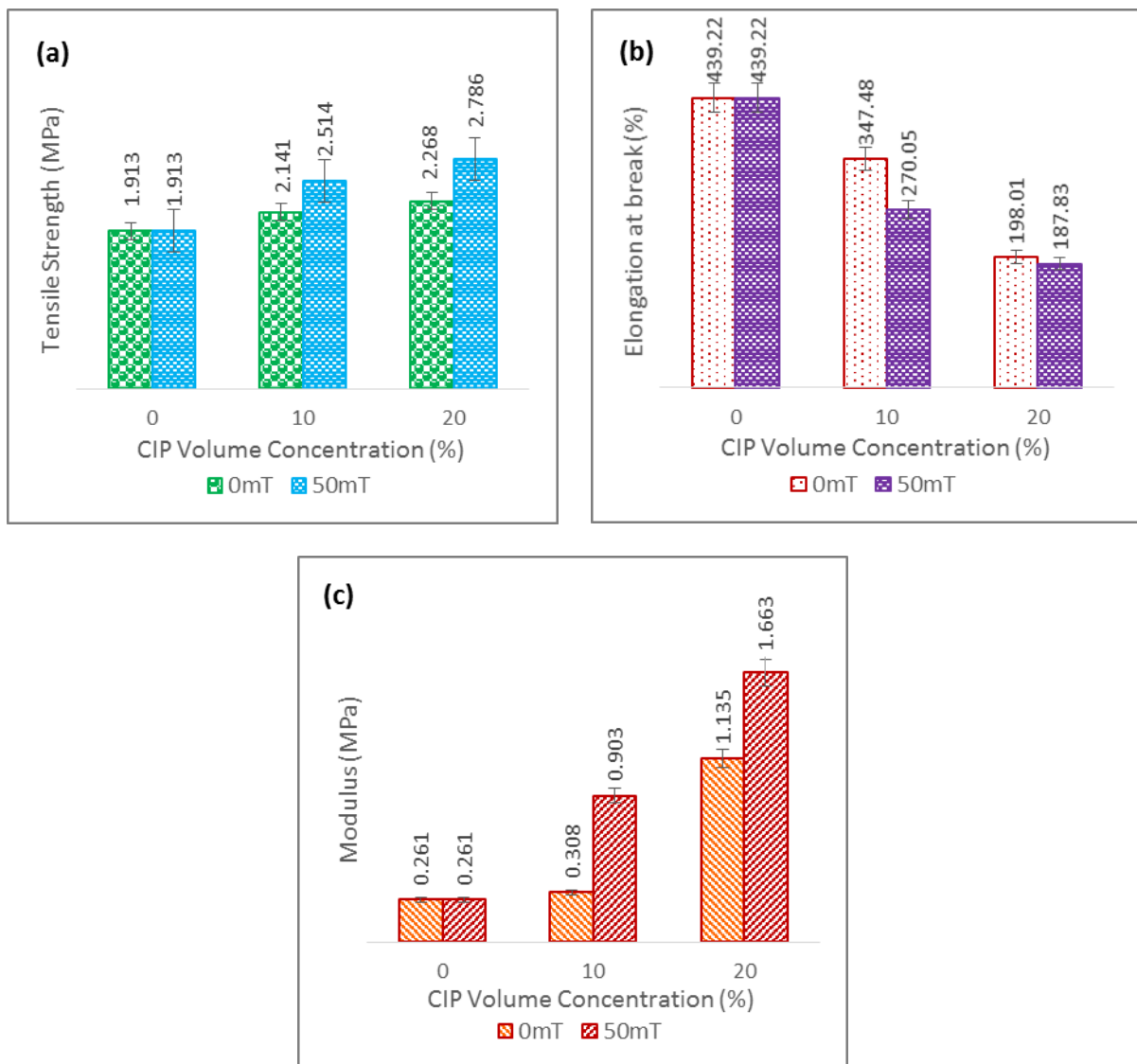


**Figure 4.** Graphs of (a) tensile strength, (b) elongation at break, and (c) engineering modulus of pure SR and anisotropic silicone-based MREs with 10 and 20 vol.% CIPs during off-state (0 mT) and on-state (50 mT) conditions.

The morphological evaluation revealed that the CIPs were well embedded and bonded in the silicone matrix prior to tensile testing of the MRE sample. However, following the tensile test, some particles spewed out of the matrix, breaking the bonds between the particles–matrix and particles–particles, resulting in the failure of the MRE samples. Figure 5c,d show the tested samples of MREs without magnetic influence (off-state) at 20 vol.% and 10 vol.%, respectively. At this stage, both MRE samples showed evidence of a failure matrix, but it was only faintly visible. Because the MRE samples were still dominated by their original elastic condition, the formation of microcracks was limited, but strain localization and microplasticity developed in very confined regions. This permanent plasticity mechanism was thought to be caused by the matrix’s amorphous molecular chain structure and cross-linkages. The MRE’s amorphous molecular chain allowed stress from external loading to be distributed evenly throughout the chain. In this case, the 50 mm/min tension loading was also important because it allowed for stress distribution per unit area of the MRE samples.

Further investigation was carried out at the MRE condition just before the breakage and when subjected to the greatest strain, as shown in Figure 6. This state represented

the Mullins effect on the sample, and this would be the only image associated with this phenomenon that has ever been reported. On Mullins' finding, microcracks and microplasticity were clearly visible in the image, and the process for their formation agreed with the literature's hypothesis [23].

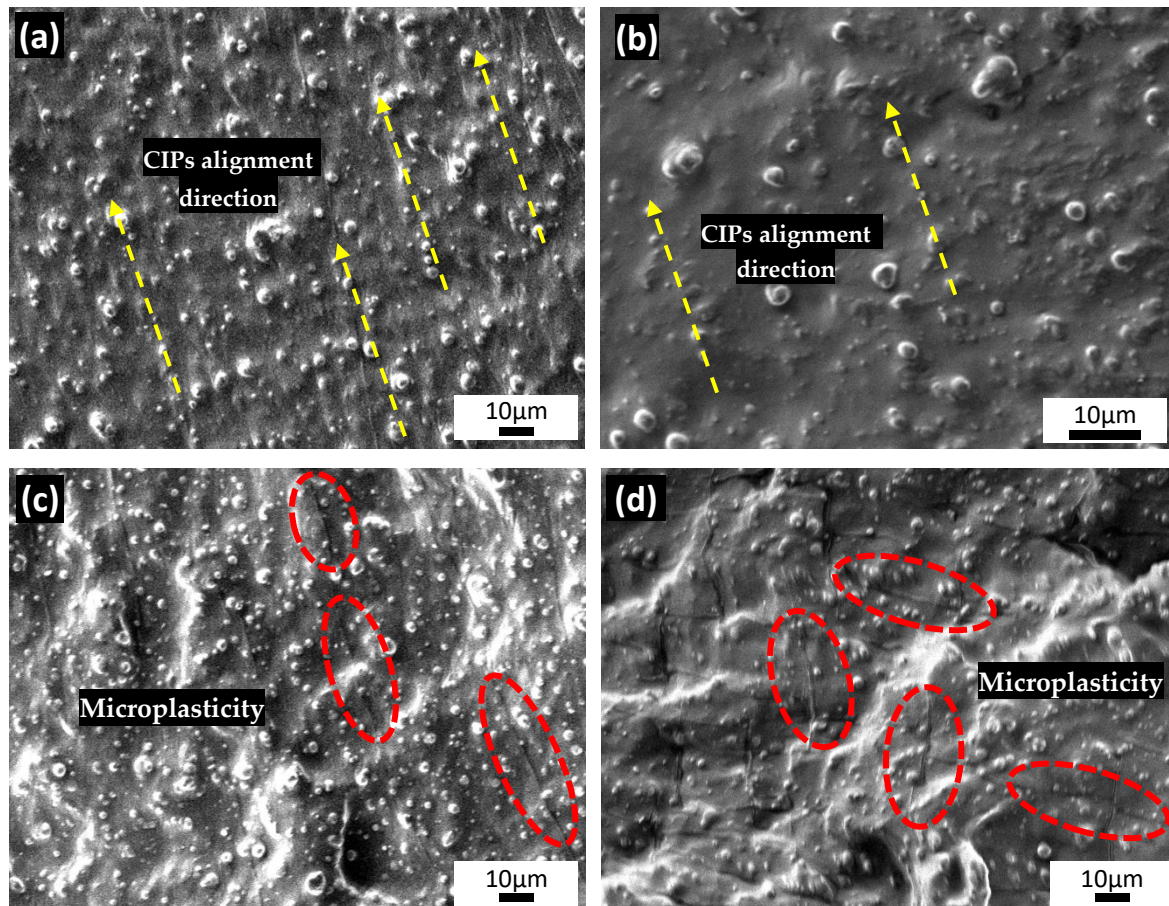


**Figure 5.** FESEM images for anisotropic MRE with particle alignment of (a) 20 vol.%, and (b) 10 vol.%, and microplasticity formation on (c) 20 vol.% and (d) 10 vol.% CIPs.

The microplasticity was essentially formed by residual stresses at a localized area, which then promoted microphase separation and chain disentanglement, leaving the microplasticity bands. Cracks in MRE samples were difficult to form due to their high elasticity and ability to store energy during formation caused by the applied force. Apparently, the hairline cracks or microcracks in the figures could have formed just before the sample break within the gauge length that occurred in the stress concentration area. At this point, the localized area was thought to have a weaker amorphous molecular structure chain and continuous applied stress, resulting in molecular slippage and, eventually, matrix bond rupture.

Tensile loading on MRE samples under magnetic field influence, on the other hand, resulted in larger cracks, as shown in Figure 7a,b. Tension load at 50 mT of external magnetic inducement stiffened the samples and promoted brittle failure at the gauge length. External magnetic inducement decreased the ability of the matrix's molecular chain, allowing less stress to be distributed in the sample. Simultaneously, the ability of deformation to store energy was reduced, hastening the microcrack formation process. The size of the microcrack significantly increased before the separation of the matrix at the concentration area within the gauge length, as the crack was triggered earlier. Both CIP



concentrations showed brittle failure in the raging zone, which was most noticeable in the MRE 20 vol.% sample.

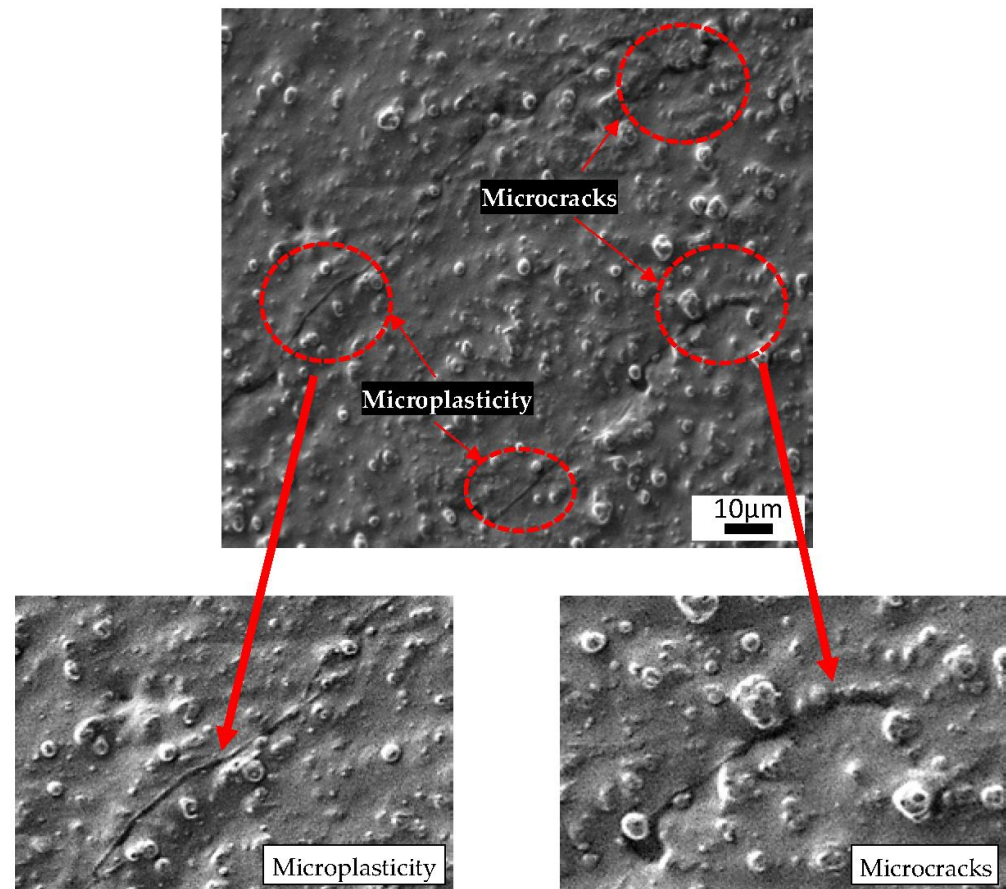


Figure 6. FESEM images of an MRE sample at maximum strain before breakage.

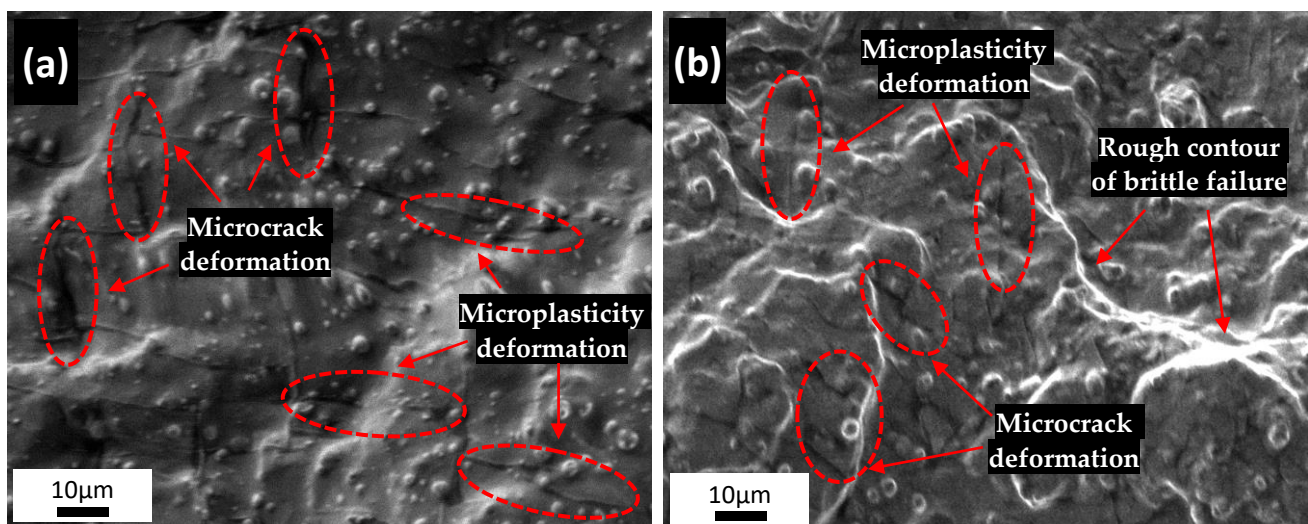


Figure 7. FESEM images of an MRE sample at tension loading under magnetic influence at CIP concentrations of MREs with (a) 10 vol.% and (b) 20 vol.%.

During the on-state condition, MRE samples exhibited greater permanent microcrack deformation and rough surfaces. There was also evidence of microplasticity bands with larger dimensions when compared to tension failures that were not magnetically influenced.

This is because the magnetic fields improved particle interaction, increasing the stiffness of the matrix. Overall, the findings of this morphological study successfully demonstrated the influence of CIP concentrations and magnetic field on the large strain behavior of anisotropic MREs as well as failure microstructure analysis for the development of material quality and performance.

### 3.3. Failure Mechanism under Tension

As previously stated, the softening effect, also known as the Mullins phenomenon, may have an impact on MRE samples, particularly the molecular structure. As a result of understanding the microstructure characteristics obtained from the morphological analysis, a proper mechanism could be proposed to further understand the phenomenon, thereby improving the effect to the test method as early as the fabrication stage. Figure 8 depicts the material softening caused by the Mullins effect, indicating that the comparability evaluation of MREs under tension load corresponds to the mechanisms underlying it during the early stage (Stage 1), maximum interval (Stage 2), and failure condition (Stage 3).

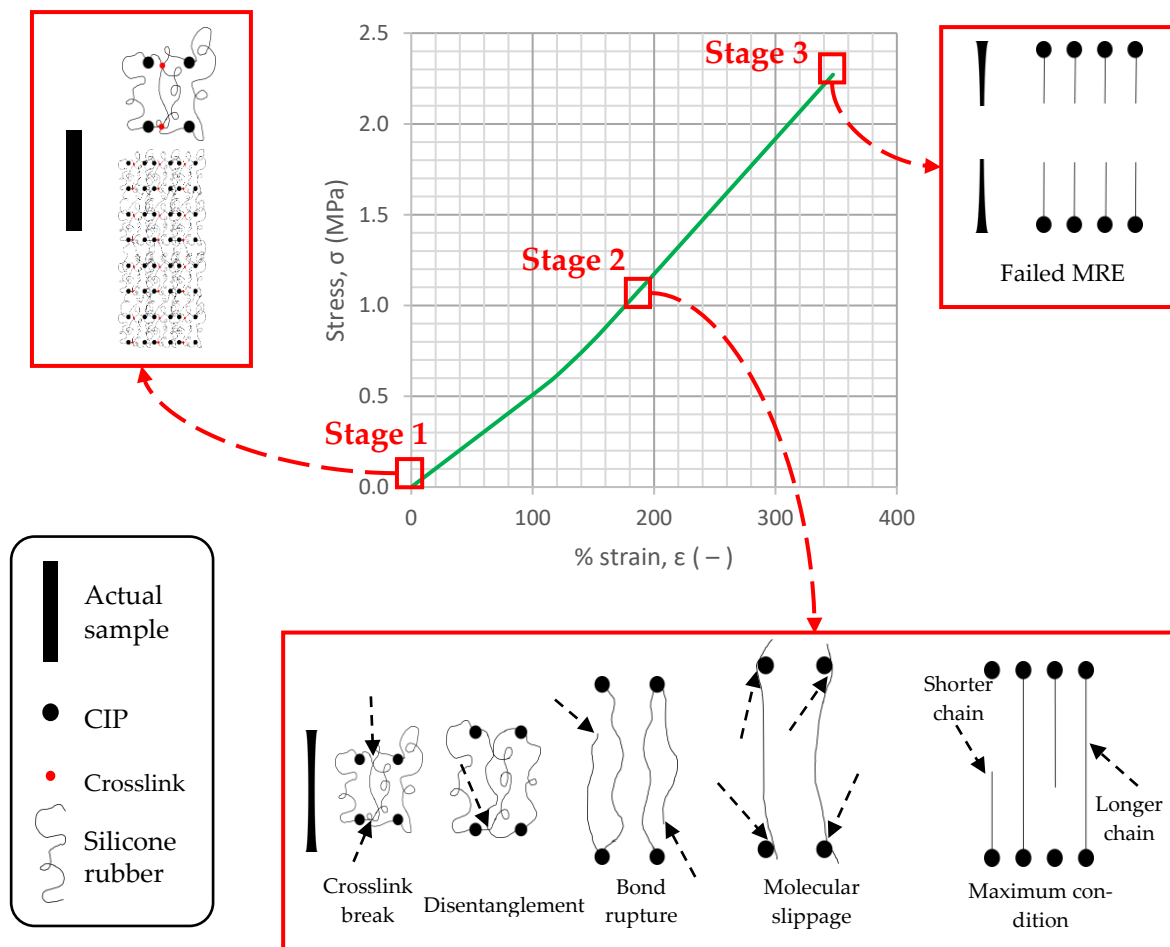


**Figure 8.** The mechanism underlying the stress–strain behavior of anisotropic silicone-based MREs with 10 vol.% CIP concentrations at off-state condition.

Beginning at Stage 1, MREs initially exhibited traditional rubber-like properties with the formation of entangled long-chain molecules and the formation of several chemical crosslinks as a result of the curing process. For its matrix amorphous molecular structure, the theoretical concept of molecular chain structure and cross-linkages in amorphous solid was ideally relevant to MRE evaluation. Crosslinks demonstrated material elasticity and deformation limitation. These crosslinks were a critical structural element that provided the

MRE system with excellent elastic properties, while also increasing rigidity and preventing viscous dominance. Furthermore, because MREs contained CIPs, there was a rubber–particle attachment, which provided restrictions in the crosslinked rubber network, known as secondary interaction [5].

Once tension stress was applied to the MREs and they began to stretch, the stress was distributed across the rubber’s molecular structures. This was classified as Stage 2, and at this stage, an interesting observation was made and proposed for the relationship with the Mullins effect. The long chain of entangled chains began to disentangle and stretch in the direction of the stress. The shorter chain and some of the crosslinking, on the other hand, began to break and disappear. During this phase, molecules began to slip over the surface of the filler, creating new bonds along the chains in an instant. As more molecular bonds ruptured, particles slipped and crosslinking disappeared, and the molecular structure of the MRE became insufficiently reconfigurable, resulting in permanent deformation. These processes and mechanisms were established and reported here in accordance with previous literature on rubber materials [23] and MREs [5]. The concept of softening in the Mullins effect has a behavior similar to studies in which stress was distributed to the region applied with tension loading. The varied stress region in Stage 2 was forced to remain localized, leading to the development of permanent microplasticity. The formation of microplasticity bands reduced the structure’s elasticity, and further stress application destroyed the shorter molecular structure and generated microcracks. The microcrack deformation resulted from a bond rupture and molecular slippage from similar shorter chains. Both deformations formed a soft domain, which contributed to the softening effects or Mullins’ phenomenon. Further stress application brought the sample to the final stage of Stage 2, indicating how much stress the sample can withstand before breaking and reaching Stage 3. The tensile strength of the MRE sample was determined at this stage.

#### 4. Conclusions

The anisotropic silicone-based magnetorheological elastomers were successfully fabricated with 10 and 20 vol.% CIPs and cured at room temperature. A pure silicon rubber with no particles added was also successfully fabricated as a reference. The mechanical properties of the samples under tension mode as well as the microstructure behavior of the failed MRE samples were thoroughly investigated and discussed. When the mechanical properties of pure silicon rubber samples were compared to silicone-based MRE samples, the tensile strength decreased as the CIP contents increased from 0 to 10 and 20 vol.%. Nonetheless, an increase in CIP contents resulted in a 350% increase in elastic modulus and simultaneously had a significant influence on the stress–strain behavior of MREs. The application of a magnetic field during the on-state condition increased particle interaction and cross-linking, resulting in increases in tensile strength, elongation at break, and elastic modulus. However, the higher CIP concentrations in MRE samples of 20 vol.% caused the MRE samples to be more brittle, resulting in a much lower increment of the similar parameters. The magnetic force applied during tension mode was critical in indicating the behavior and characteristics of the MRE failure mechanism, particularly at high strain, contributing to the new knowledge of MREs in tension mode. This study provided valuable insight into the MRE morphology of tensile failure and made a significant contribution to the scientific evidence of the Mullins effect on microstructural behavior. Thus, it can be concluded that the concentration of CIPs has a significant effect on the mechanical properties of MREs in the quasi-static tensile condition; this has the potential to be investigated further in MREs subjected to cyclic or dynamic loading conditions.

**Author Contributions:** S.F.M.S.: writing—original draft preparation, methodology, investigation; S.A.M.: supervision, conceptualization, writing—reviewing and editing; N.J.: supervision, writing—reviewing and editing; M.A.F.J.: writing—reviewing and editing, methodology, investigation, validation; S.A.A.A.: writing—reviewing and editing; M.H.A.K.: writing—reviewing and editing; N.A.N.: writing—reviewing and editing; N.M.H.: writing—reviewing and editing. All authors participated in writing the manuscript. All authors have read and agreed to the published version of the manuscript.

**Funding:** This research was funded by UTM Fundamental Research (Vot No. 22H14) and Professional Development Research University (PDRU) (Vot. No. 06E29).

**Data Availability Statement:** The raw/processed data required to reproduce these findings cannot be shared at this time as the data also form part of an ongoing study. In the future, however, the raw data required to reproduce these findings will be available from the corresponding authors.

**Conflicts of Interest:** The authors declare no conflict of interest.

## References

1. Ubaidillah; Sutrisno, J.; Purwanto, A.; Mazlan, S.A. Recent Progress on Magnetorheological Solids: Materials, Fabrication, Testing, and Applications. *Adv. Eng. Mater.* **2015**, *17*, 563–597. [[CrossRef](#)]
2. Sandesh, B.; Sriharsha, H.; Rao Sathish, U.; Nikhil, G. Investigation of Tensile Properties of RTV Silicone Based Isotropic Magnetorheological Elastomers. *MATEC Web. Conf.* **2018**, *144*, 02015. [[CrossRef](#)]
3. Faizal Johari, M.A.; Mazlan, S.A.; Ubaidillah; Harjana; Abdul Aziz, S.A.; Nordin, N.A.; Johari, N.; Nazmi, N. An Overview of Durability Evaluations of Elastomer-Based Magnetorheological Materials. *IEEE Access* **2020**, *8*, 134536–134552. [[CrossRef](#)]
4. Abd Rashid, R.Z.; Johari, N.; Mazlan, S.A.; Abdul Aziz, S.A.; Nordin, N.A.; Nazmi, N.; Aqida, S.N.; Johari, M.A.F. Effects of Silica on Mechanical and Rheological Properties of EPDM-Based Magnetorheological Elastomers. *Smart Mater. Struct.* **2021**, *30*, 105033. [[CrossRef](#)]
5. Johari, M.A.F.; Mazlan, S.A.; Nasef, M.M.; Ubaidillah, U.; Nordin, N.A.; Aziz, S.A.A.; Johari, N.; Nazmi, N. Microstructural Behavior of Magnetorheological Elastomer Undergoing Durability Evaluation by Stress Relaxation. *Sci. Rep.* **2021**, *11*, 10936. [[CrossRef](#)]
6. Aziz, S.A.A.; Mazlan, S.A.; Ismail, N.I.N.; Ubaidillah, U.; Choi, S.B.; Khairi, M.H.A.; Yunus, N.A. Effects of Multiwall Carbon Nanotubes on Viscoelastic Properties of Magnetorheological Elastomers. *Smart Mater. Struct.* **2016**, *25*, 077001. [[CrossRef](#)]
7. Khairi, M.H.A.; Fatah, A.Y.A.; Mazlan, S.A.; Ubaidillah, U.; Nordin, N.A.; Ismail, N.I.N.; Choi, S.B.; Aziz, S.A.A. Enhancement of Particle Alignment Using Silicone Oil Plasticizer and Its Effects on the Field-Dependent Properties of Magnetorheological Elastomers. *Int. J. Mol. Sci.* **2019**, *20*, 4085. [[CrossRef](#)]
8. Burhannuddin, N.L.; Nordin, N.A.; Mazlan, S.A.; Abdul Aziz, S.A.; Choi, S.B.; Kuwano, N.; Nazmi, N.; Johari, N. Effects of Corrosion Rate of the Magnetic Particles on the Field-Dependent Material Characteristics of Silicone Based Magnetorheological Elastomers. *Smart Mater. Struct.* **2020**, *29*, 087003. [[CrossRef](#)]
9. Zhang, G.; Zhang, J.; Guo, X.; Zhang, M.; Liu, M.; Qiao, Y.; Zhai, P. Effects of Graphene Oxide on Microstructure and Mechanical Properties of Isotropic Polydimethylsiloxane-Based Magnetorheological Elastomers. *Rheol. Acta* **2022**, *61*, 215–228. [[CrossRef](#)]
10. Kumar, V.; Lee, D.J. Iron Particle and Anisotropic Effects on Mechanical Properties of Magneto-Sensitive Elastomers. *J. Magn. Magn. Mater.* **2017**, *441*, 105–112. [[CrossRef](#)]
11. Schubert, G.; Harrison, P. Large-Strain Behaviour of Magneto-Rheological Elastomers Tested under Uniaxial Compression and Tension, and Pure Shear Deformations. *Polym. Test.* **2015**, *42*, 122–134. [[CrossRef](#)]
12. Norouzi, M.; Gilani, M.; Alehashem, S.M.S.; Vatandoost, H. Dynamic Characterization and Modeling of Isotropic Magnetorheological Elastomers under Tensile-Compressive Loadings. *IEEE Trans. Magn.* **2017**, *53*, 2900412. [[CrossRef](#)]
13. Soria-hern, C.G.; Palacios-pineda, L.M.; Elias-Zuniga, A.; Perales-Martínez, I.A.; Martínez-Romero, O. Investigation of the Effect of Carbonyl Iron Micro-Particles on the Mechanical and Rheological Properties of Isotropic and Anisotropic MREs: Constitutive Magneto-Mechanical Material Model. *Polymers* **2019**, *11*, 1705. [[CrossRef](#)] [[PubMed](#)]
14. Gorman, D.; Murphy, N.; Ekins, R.; Jerrams, S. The Evaluation and Implementation of Magnetic Fields for Large Strain Uniaxial and Biaxial Cyclic Testing of Magnetorheological Elastomers. *Polym. Test.* **2016**, *51*, 74–81. [[CrossRef](#)]
15. Kumar, V.; Alam, M.N.; Park, S.S. Soft Composites Filled with Iron Oxide and Graphite Nanoplatelets under Static and Cyclic Strain for Different Industrial Applications. *Polymers* **2022**, *14*, 2393. [[CrossRef](#)]
16. Qiao, Y.; Zhang, J.; Zhang, M.; Liu, L.; Zhai, P. A Magneto-Hyperelastic Model for Silicone Rubber-Based Isotropic Magnetorheological Elastomer under Quasi-Static Compressive Loading. *Polymers* **2020**, *12*, 2435. [[CrossRef](#)]
17. Vatandoost, H.; Sedaghati, R.; Rakheja, S.; Hemmatian, M. Effect of Pre-Strain on Compression Mode Properties of Magnetorheological Elastomers. *Polym. Test.* **2021**, *93*, 106888. [[CrossRef](#)]
18. Johari, M.A.F.; Mazlan, S.A.; Nordin, N.A.; Ubaidillah, U.; Aziz, S.A.A.; Nazmi, N.; Johari, N.; Choi, S.B. The Effect of Microparticles on the Storage Modulus and Durability Behavior of Magnetorheological Elastomer. *Micromachines* **2021**, *12*, 948. [[CrossRef](#)]
19. Gao, P.; Liu, H.; Xiang, C.; Yan, P.; Mahmoud, T. A New Magnetorheological Elastomer Torsional Vibration Absorber: Structural Design and Performance Test. *Mech. Sci.* **2021**, *12*, 321–332. [[CrossRef](#)]
20. Akif, M.; Fakhree, M.; Nordin, N.A.; Nazmi, N.; Mazlan, S.A.; Aishah, S.; Aziz, A.; Ubaidillah, U.; Ahmad, F.; Choi, S. Field-Dependent Rheological Properties of Magnetorheological Elastomer with Fountain-Like Particle Chain Alignment. *Micromachines* **2022**, *13*, 492.
21. Khairi, M.H.A.; Mazlan, S.A.; Ubaidillah; Nordin, N.A.; Aziz, S.A.A.; Nazmi, N. Effect of Mould Orientation on the Field-Dependent Properties of Mr Elastomers under Shear Deformation. *Polymers* **2021**, *13*, 3273. [[CrossRef](#)] [[PubMed](#)]

22. El-Atab, N.; Mishra, R.B.; Al-Modaf, F.; Joharji, L.; Alsharif, A.A.; Alamoudi, H.; Diaz, M.; Qaiser, N.; Hussain, M.M. Soft Actuators for Soft Robotic Applications: A Review. *Adv. Intell. Syst.* **2020**, *2*, 128. [[CrossRef](#)]
23. Diani, J.; Fayolle, B.; Gilormini, P. A Review on the Mullins Effect. *Eur. Polym. J.* **2009**, *45*, 601–612. [[CrossRef](#)]
24. Wei, C.; Wang, J.; He, Y.; Li, J.; Beaugnon, E. Solidification of Immiscible Alloys under High Magnetic Field: A Review. *Metals* **2021**, *11*, 525. [[CrossRef](#)]
25. Milyutin, V.A.; Gervasyeva, I.V. Thermally Activated Transformations in Alloys with Different Type of Magnetic Ordering under High Magnetic Field. *J. Magn. Magn. Mater.* **2019**, *492*, 165654. [[CrossRef](#)]
26. Xiang, Z.; Zhang, L.; Xin, Y.; An, B.; Niu, R.; Mardani, M.; Siegrist, T.; Lu, J.; Goddard, R.E.; Man, T.; et al. Ultrafine Microstructure and Hardness in Fe-Cr-Co Alloy Induced by Spinodal Decomposition under Magnetic Field. *Mater. Des.* **2021**, *199*, 109383. [[CrossRef](#)]
27. Han, K.; Zhou, X. Effect of High Magnetic Field on the Processing of Pearlitic Steels. *Mater. Manuf. Process.* **2017**, *32*, 1317–1324. [[CrossRef](#)]
28. Zuo, X.; Zhang, L.; Wang, E. Influence of External Static Magnetic Fields on Properties of Metallic Functional Materials. *Crystals* **2017**, *7*, 374. [[CrossRef](#)]
29. Boczkowska, A.; Awietj, S. Microstructure and Properties of Magnetorheological Elastomers. In *Advanced Elastomers—Technology, Properties and Applications*; InTech: Rijeka, Croatia, 2012.
30. Lai, N.T.; Ismail, H.; Abdullah, M.K.; Shuib, R.K. Optimization of Pre-Structuring Parameters in Fabrication of Magnetorheological Elastomer. *Arch. Civ. Mech. Eng.* **2019**, *19*, 557–568. [[CrossRef](#)]
31. Boczkowska, A.; Awietjan, S.F.; Wejrzanowski, T.; Kurzydłowski, K.J. Image Analysis of the Microstructure of Magnetorheological Elastomers. *J. Mater. Sci.* **2009**, *44*, 3135–3140. [[CrossRef](#)]
32. Chen, L.; Gong, X.L.; Li, W.H. Microstructures and Viscoelastic Properties of Anisotropic Magnetorheological Elastomers. *Smart Mater. Struct.* **2007**, *16*, 2645. [[CrossRef](#)]
33. Damiani, R.; Sun, L.Z. Microstructural Characterization and Effective Viscoelastic Behavior of Magnetorheological Elastomers with Varying Acetone Contents. *Int. J. Damage Mech.* **2017**, *26*, 104–118. [[CrossRef](#)]
34. Liao, G.; Gong, X.L.; Xuan, S. Influence of Shear Deformation on the Normal Force of Magnetorheological Elastomer. *Mater. Lett.* **2013**, *106*, 270–272. [[CrossRef](#)]
35. Johari, M.A.F.; Mazlan, S.A.; Ubaidillah; Nordin, N.A.; Aziz, S.A.A.; Johari, N.; Nazmi, N.; Homma, K. Shear Band Formation in Magnetorheological Elastomer under Stress Relaxation. *Smart Mater. Struct.* **2021**, *30*, 045015. [[CrossRef](#)]
36. Guan, X.; Dong, X.; Ou, J. Magnetostrictive Effect of Magnetorheological Elastomer. *J. Magn. Magn. Mater.* **2008**, *320*, 158–163. [[CrossRef](#)]